

International Journal of Modern Physics E  
© World Scientific Publishing Company

## Short Distance Repulsion Among Baryons

SINYA AOKI\*

*Graduate School of Pure and Applied Sciences, University of Tsukuba, Ten-oh-dai 1-1-1  
Tsukuba, Ibaraki 305-8571, Japan  
saoki@het.ph.tsukuba.ac.jp*

JANOS BALOG

*Institute for Particle and Nuclear Physics, Wigner Research Centre for Physics, H-1525  
Budapest 114, P.O.B. 49, Hungary  
balog.janos@wigner.mta.hu*

TAKUMI DOI

*Theoretical Research Division, Nishina Center, RIKEN  
Wako 351-0198, Japan  
doi@ribf.riken.jp*

TAKASHI INOUE

*Nihon University, College of Bioresource Sciences  
Kanagawa 252-0880, Japan  
inoue.takashi@nihon-u.ac.jp*

PETER WEISZ

*Max-Planck-Institut für Physik, Föhringer Ring 6,  
D-80805 München, Germany  
pew@mpp.mpg.de*

Received Day Month Year

Revised Day Month Year

We review recent investigations on the short distance behaviors of potentials among baryons, which are formulated through the Nambu-Bethe-Salpeter (NBS) wave function. After explaining the method to define the potentials, we analyze the short distance behavior of the NBS wave functions and the corresponding potentials by combining the OPE (operator product expansion) and a renormalization group analysis in the perturbation theory of QCD. These analytic results are compared with numerical results obtained in lattice QCD simulations.

*Keywords:* baryon interaction; repulsive core; operator product expansion; lattice QCD.

PACS numbers: 12.38.Gc, 12.38.Bx, 13.75.-n, 21.30.-x

\*Address after April 1, 2013: Yukawa Institute for Theoretical Physics, Kyoto University, Kitashirakawa Oiwakecho, Sakyo-ku, Kyoto 606-8502, Japan

2 *S. Aoki, J. Balog, T. Doi, T. Inoue, P. Weisz*

## 1. Introduction

A force between nucleons, the nuclear force, is the most fundamental quantity in nuclear physics. The phenomenological nucleon-nucleon (NN) potentials<sup>1</sup> exhibit long-to-medium distance attractions, which have been explained by meson exchanges between nucleons,<sup>2</sup> while they have short distance repulsion, the repulsive core,<sup>3</sup> essential for the stability of nuclei against collapse, whose origin has not yet been well understood. Moreover, general short distance repulsions among baryons, not only NN but also three-nucleon (3N), baryon-baryon (BB) and three-baryon (3B),<sup>4</sup> may be required to explain a recently observed<sup>5</sup> neutron star as heavy as twice a solar mass. Unfortunately it is difficult or almost impossible to determine these short distance repulsions experimentally, except for the NN case, while the theoretical determination for these short distance repulsions requires difficult non-perturbative calculations in QCD.

Recently, a novel method to define the NN potential in QCD has been proposed<sup>6–8</sup> (we call it the HAL QCD scheme or method in this paper), and the method has been widely applied to various hadronic interactions<sup>9–14</sup> including BB potentials<sup>15,16</sup> and 3N forces.<sup>17</sup> Furthermore, in the HAL QCD scheme, the short distance behavior of two- and three baryon potentials can be investigated analytically via the operator product expansion combined with a renormalization group (RG) analysis of perturbative QCD.<sup>18–22</sup>

In this paper, we review both analytical investigations and numerical results for short distance behaviors of these potentials in the HAL QCD method. In Sec. 2 we briefly explain the HAL QCD method to define the potential in QCD, taking the NN case as an example. The OPE (operator product expansion) formalism to analyze the short distance behaviors of potentials in the HAL QCD scheme is summarized in Sec. 3. Results for potentials in lattice QCD simulations are summarized and compared with the OPE analyses in Sec. 4, and a summary is given in Sec. 5.

## 2. HAL QCD method

In this section, we explain the HAL QCD method to define the potential in QCD for the NN case. The basic quantity is the equal-time Nambu-Bethe-Salpeter(NBS) wave function, defined by

$$\varphi_{\alpha\beta}^{\mathbf{k},s_1s_2}(\mathbf{x}) = \langle 0|T\{N_\alpha(\mathbf{x}_0,0)N_\beta(\mathbf{x}_0+\mathbf{x},0)\}|NN,\mathbf{k},s_1s_2\rangle_{\text{in}}, \quad (1)$$

where  $\langle 0|$  is the QCD vacuum (bra)-state,  $|NN,\mathbf{k},s_1s_2\rangle_{\text{in}}$  is the two-nucleon asymptotic in-state with helicity  $s_1, s_2$  and relative momentum  $\mathbf{k}$  in the center of mass frame, whose total energy is given by  $W_{\mathbf{k}} = 2\sqrt{\mathbf{k}^2 + m_N^2}$  with the nucleon mass  $m_N$ , and  $T$  represents the time-ordered product. The local interpolating operator for the nucleon is taken as  $N_\alpha(x) = \varepsilon_{abc}(u^a(x)^T C \gamma_5 d^b(x)) q_\alpha^c(x)$  (with  $x = (\mathbf{x}, t)$ ), where  $a, b, c$  are the color indices,  $\alpha$  is the spinor index,  $C = \gamma_2 \gamma_4$  is the charge conjugation matrix, and  $q(x) = (u(x), d(x))$ .

As long as the total energy  $W_{\mathbf{k}}$  lies below the pion production threshold (*i.e.*  $W_{\mathbf{k}} < W_{\text{th}} = 2m_N + m_\pi$  with pion mass  $m_\pi$ ), the NBS wave function at  $r = |\mathbf{x}| \rightarrow \infty$  satisfies the Helmholtz equation:

$$[k^2 + \nabla^2] \varphi_{\Gamma}^{\mathbf{k},c}(\mathbf{x}) \simeq 0, \quad k = |\mathbf{k}|, \quad (2)$$

where  $c \equiv s_1 s_2$  and  $\Gamma \equiv \alpha\beta$ . Moreover, the radial part of the NBS wave function for given orbital angular momentum  $L$  and total spin  $S$  for asymptotically large  $r$  becomes<sup>8,23</sup>

$$\varphi^{\mathbf{k}}(r; LS) \propto \frac{\sin(kr - L\pi/2 + \delta_{LS}(k))}{kr} e^{i\delta_{LS}(k)}, \quad (3)$$

where  $\delta_{LS}(k)$  is the NN phase shift obtained from the S-matrix in QCD below the inelastic threshold.

From the above property of the NBS wave function, it is possible to define a non-local potential through the equation

$$[E_k - H_0] \varphi_{\Gamma}^{\mathbf{k},c}(\mathbf{x}) = \sum_{\Gamma_1} \int U_{\Gamma;\Gamma_1}(\mathbf{x}, \mathbf{y}) \varphi_{\Gamma_1}^{\mathbf{k},c}(\mathbf{y}) d^3 y, \quad \left( E_k = \frac{k^2}{2\mu}, \quad H_0 = -\frac{\nabla^2}{2\mu} \right) \quad (4)$$

with the reduced mass  $\mu = m_N/2$ , where  $U(\mathbf{x}, \mathbf{y})$  is expected to be short-ranged because of absence of massless particle exchanges between two nucleons. The potential  $U(\mathbf{x}, \mathbf{y})$  is finite and does not depend on the particular renormalization scheme, since the NBS wave function  $\varphi_{\alpha\beta}^{\mathbf{k},c}$  is multiplicatively renormalized. While Lorentz covariance is lost by using the equal-time NBS wave function and Eq. (4) is written as a Schrödinger type equation, a non-relativistic "approximation" is NOT introduced to define  $U(\mathbf{x}, \mathbf{y})$ .

The non-local but energy( $\mathbf{k}$ )-independent potential  $U(\mathbf{x}, \mathbf{y})$  can be formally given by,<sup>7,8</sup>

$$U_{\Gamma_1, \Gamma_2}(\mathbf{x}, \mathbf{y}) = \sum_{\mathbf{k}_1, c_1; \mathbf{k}_2, c_2}^{|\mathbf{k}_1|, |\mathbf{k}_2| < k_{\text{th}}} [E_{k_1} - H_0] \varphi_{\Gamma_1}^{\mathbf{k}_1, c_1}(\mathbf{x}) \mathcal{N}_{\mathbf{k}_1, c_1; \mathbf{k}_2, c_2}^{-1} \varphi_{\Gamma_2}^{\mathbf{k}_2, c_2}(\mathbf{y})^\dagger, \quad (5)$$

where  $k_{\text{th}}$  is the threshold momentum defined to satisfy  $2\sqrt{k_{\text{th}}^2 + m_N^2} = W_{\text{th}}$  so that the summation over  $\mathbf{k}_1, \mathbf{k}_2$  is restricted below the inelastic threshold, and  $\mathcal{N}^{-1}$  is the inverse of  $\mathcal{N}$  defined from the inner product of NBS wave functions as

$$\mathcal{N}^{\mathbf{k}_1, c_1; \mathbf{k}_2, c_2} = (\varphi^{\mathbf{k}_1, c_1}, \varphi^{\mathbf{k}_2, c_2}) \equiv \sum_{\Gamma} \int d^3 x \varphi_{\Gamma}^{\mathbf{k}_1, c_1}(\mathbf{x})^\dagger \varphi_{\Gamma}^{\mathbf{k}_2, c_2}(\mathbf{x}) \quad (6)$$

for  $|\mathbf{k}_1|, |\mathbf{k}_2| < k_{\text{th}}$ . This  $U(\mathbf{x}, \mathbf{y})$  is energy-independent by construction and satisfies eq. (4) as

$$\begin{aligned} \sum_{\Gamma_1} \int U_{\Gamma;\Gamma_1}(\mathbf{x}, \mathbf{y}) \varphi_{\Gamma_1}^{\mathbf{k},c}(\mathbf{y}) d^3 y &= \sum_{\mathbf{k}_1, c_1; \mathbf{k}_2, c_2}^{|\mathbf{k}_1|, |\mathbf{k}_2| < k_{\text{th}}} [E_{k_1} - H_0] \varphi_{\Gamma}^{\mathbf{k}_1, c_1}(\mathbf{x}) \mathcal{N}_{\mathbf{k}_1, c_1; \mathbf{k}_2, c_2}^{-1} \cdot \mathcal{N}^{\mathbf{k}_2, c_2; \mathbf{k}, c} \\ &= [E_k - H_0] \varphi_{\Gamma}^{\mathbf{k},c}(\mathbf{x}) \end{aligned} \quad (7)$$

4 *S. Aoki, J. Balog, T. Doi, T. Inoue, P. Weisz*

as long as  $W_{\mathbf{k}} < W_{\text{th}}$ . Once the non-local potential  $U(\mathbf{x}, \mathbf{y})$  which satisfies eq. (4) is obtained, eq. (3) guarantees that we can extract the phase shift  $\delta_{LS}(k)$  at  $W_{\mathbf{k}} < W_{\text{th}}$  in QCD by solving the Schrödinger equation with this potential. Note however that the non-local potential which satisfies eq. (4) at  $W_{\mathbf{k}} < W_{\text{th}}$  is not unique, since the potential itself is not a physical observable. We may add terms orthogonal to all NBS wave functions below the inelastic threshold, which only affect eq. (4) at  $W_{\mathbf{k}} \geq W_{\text{th}}$ .<sup>8</sup>

The construction of  $U(\mathbf{x}, \mathbf{y})$  in eq. (5) is formal and is inadequate for practical use, since only a limited number of wave functions at low energies (ground state and possibly a few low-lying excited states) can be obtained in lattice QCD simulations in a finite box. In practice, we therefore expand the non-local potential in terms of the velocity (derivative) with local coefficient functions;<sup>24</sup>  $U(\mathbf{x}, \mathbf{y}) = V(\mathbf{x}, \nabla)\delta^3(\mathbf{x} - \mathbf{y})$ , whose leading order terms reads

$$V^{\text{LO}}(\mathbf{x}) = V_0(r) + V_\sigma(r)\boldsymbol{\sigma}_1 \cdot \boldsymbol{\sigma}_2 + V_T(r)S_{12}, \quad (8)$$

where  $\boldsymbol{\sigma}_i$  is the Pauli-matrix acting on the spin index of the  $i$ -th nucleon, and  $S_{12} = 3(\mathbf{x} \cdot \boldsymbol{\sigma}_1)(\mathbf{x} \cdot \boldsymbol{\sigma}_2)/r^2 - \boldsymbol{\sigma}_1 \cdot \boldsymbol{\sigma}_2$  is the tensor operator. It has been found in numerical simulations<sup>10</sup> that contributions from higher order terms are much smaller than those from  $V^{\text{LO}}$  at low energy. This means that non-locality is rather small at low energy in our definition of the potential.

For example for  $L = 0$  and  $S = 0$ , we obtain

$$V_C(r, L = S = 0) \equiv V_0(r) - 3V_\sigma(r) = \frac{(E_k - H_0)\varphi^{\mathbf{k},c}(r, L = S = 0)}{\varphi^{\mathbf{k},c}(r, L = S = 0)}. \quad (9)$$

As mentioned before, since the potential itself is not a physical observable, its short-distance behavior depends on its definition, in particular, the choice of nucleon operator in the NBS wave function. In this review, we analyze the short distance behaviors of the potentials defined in the HAL QCD scheme exclusively, by comparing analytic results to numerical results from lattice QCD simulations. The method in this review, however, can be easily applied to other definitions for the potential.

### 3. OPE and short distance behavior of the potential

#### 3.1. Notation and Method

One of the outstanding properties of QCD is asymptotic freedom; renormalized running couplings  $\bar{g}^2(r)$  which characterize interactions at short distance scales  $r$  tend logarithmically to zero as the scale decreases  $\bar{g}^2(r) \sim -\frac{1}{2\beta_0 \ln(\Lambda r)}$ , where  $\beta_0 = [11 - 2N_f/3]/(16\pi^2)$  for gauge group SU(3), provided the number of dynamical quarks is limited ( $N_f \leq 16$ ). This has the important consequence that the behavior of a wide class of physical quantities at short distances (alternatively high energies) can be computed perturbatively. The NBS wave functions defined in eq. (1) belong to this class. In the framework of perturbation theory of QCD it is convenient to

regularize the ultra-violet divergences using dimensional regularization (DR), and then bare parameters and operators must be renormalized.

The operator product expansion (OPE) method is based on the observation that the product of the two renormalized nucleon operators appearing in the definition of the NBS wave function is for short distances expressed as a sum of local gauge invariant operators times coefficient functions:

$$N_\alpha(0,0)N_\beta(\mathbf{x},0) \underset{\mathbf{x} \rightarrow 0}{\sim} \sum_A F_{\alpha\beta}^A(\mathbf{x})\mathcal{O}_A, \quad (10)$$

which holds when sandwiched between asymptotic states or in correlation functions with fundamental fields at widely separated distances. The coefficient functions  $F_{\alpha\beta}^A(\mathbf{x})$  appearing above can be computed perturbatively using the RG equations which express independence of the bare theory on the renormalization scale.<sup>a</sup> If the nucleon operators and the  $\mathcal{O}_A$  are chosen so that they renormalize multiplicatively without mixing:  $\mathcal{O}_A = Z_A\mathcal{O}_{A,\text{bare}}$ , then the corresponding coefficients behave as  $F_{\alpha\beta}^A(\mathbf{x}) \sim \bar{g}^{2(\ell_A - \beta_A)}(|\mathbf{x}|)$ , where  $\ell_A$  determines the loop order at which the corresponding operator first appears in perturbation theory (PT) and  $\beta_A$  is related to the difference of the 1-loop anomalous dimension  $\gamma_A$  of the operator  $\mathcal{O}_A$  and that of two nucleons  $\gamma_N = 1/4\pi^2$ :  $\beta_A = (\gamma_A - 2\gamma_N)/(2\beta_0)$ .

The leading asymptotic short distance behavior of the NBS wave function is then dominated by the operator with the smallest value of  $\ell_A - \beta_A$ , provided of course that its matrix element between the vacuum and the particular 2N state does not vanish (which is generically the case). Usually the smallest value of  $\ell_A - \beta_A$  is attained for operators  $\mathcal{O}_A$  which appear at tree level ( $\ell_A = 0$ ) i.e.  $c_A \neq 0$  in the free field expansion:

$$\begin{aligned} N_{\alpha;\text{bare}}(0,0)N_{\beta;\text{bare}}(\mathbf{x},0) \underset{g_0=0}{\sim} & : N_{\alpha;\text{bare}}N_{\beta;\text{bare}} : (0,0) + \text{O}(\mathbf{x}) \\ & = \sum_B c_B \mathcal{O}_{B;\text{bare}}(0,0) + \text{O}(\mathbf{x}). \end{aligned} \quad (11)$$

Given an arbitrary basis of gauge invariant  $r$ -quark operators the anomalous dimensions are related to the eigenvalues of the matrix  $Z$  specifying the mixing under renormalization. The renormalization constant matrix can be determined by computing the correlation function of the operators multiplied by  $r$  quark fields at widely separated distances. The 1-loop computation just involves the diagrams with a gluon line connecting a pair of quark lines emanating from the operator vertex. The divergent part, using DR in  $D = 4 - 2\epsilon$  dimensions is symbolically of the form:

$$\left[ q_\alpha^{a,f}(x)q_\beta^{b,g}(x) \right]^{1-\text{loop,div}} = \frac{g^2}{96\pi^2} \frac{1}{\epsilon} [(\mathbf{T}_0 + \lambda\mathbf{T}_1) \cdot q^a(x) \otimes q^b(x)]_{\alpha,\beta}^{f,g} \quad (12)$$

where  $\mathbf{T}_0, \mathbf{T}_1$  are matrices in flavor and spinor space. The term proportional to the covariant gauge parameter  $\lambda$  cancels with the renormalization of the external

<sup>a</sup>For details we refer the reader to sect. 3 of ref.<sup>18</sup>

6 *S. Aoki, J. Balog, T. Doi, T. Inoue, P. Weisz*

quark lines. Thus only  $\mathbf{T}_0$  is relevant here, which in a chiral representation of the gamma matrices, i.e.  $\gamma_5 = \text{diag}(1, 1, -1, -1)$ , is simply given by

$$(\mathbf{T}_0)_{\alpha\alpha_1, \beta\beta_1}^{ff_1, gg_1} = \delta^{ff_1} \delta^{gg_1} [\delta_{\alpha\alpha_1} \delta_{\beta\beta_1} - 2\delta_{\beta\alpha_1} \delta_{\alpha\beta_1}] + 3\delta^{gf_1} \delta^{fg_1} [\delta_{\beta\alpha_1} \delta_{\alpha\beta_1} - 2\delta_{\alpha\alpha_1} \delta_{\beta\beta_1}] \quad (13)$$

where either  $\alpha_1, \beta_1 \in \{1, 2\}$  (right-handed) or  $\alpha_1, \beta_1 \in \{3, 4\}$  (left-handed).

Now any local gauge invariant 6-quark operator of (lowest) canonical dimension 9 can be written as a linear combination of operators of the form

$$B_{\Gamma_1, \Gamma_2}^{F_1, F_2}(x) \equiv B_{\Gamma_1}^{F_1}(x) B_{\Gamma_2}^{F_2}(x), \quad B_{\Gamma}^F(x) \equiv B_{\alpha\beta\gamma}^{fgh}(x) = \varepsilon^{abc} q_{\alpha}^{a,f}(x) q_{\beta}^{b,g}(x) q_{\gamma}^{c,h}(x), \quad (14)$$

where  $\Gamma = \{\alpha, \beta, \gamma\}$  are sets of spinor labels and  $F = \{f, g, h\}$  are sets of flavor labels.

Due to the structure of (13), which reflects the chirality conservation of massless QCD, the operators in eq. (14) mix only with operators which preserve the set of flavor and Dirac indices in the chiral basis i.e.

$$F_1 \cup F_2 = F'_1 \cup F'_2, \quad \Gamma_1 \cup \Gamma_2 = \Gamma'_1 \cup \Gamma'_2.$$

We thus start by constructing sets of operators with fixed flavor and Dirac structure. Note however that such operators are not all linearly independent. Relations between them of the form

$$3B_{\Gamma_1, \Gamma_2}^{F_1, F_2} + \sum_{i,j=1}^3 B_{(\Gamma_1, \Gamma_2)[i,j]}^{(F_1 F_2)[i,j]} = 0, \quad (15)$$

follow from an identity satisfied by the totally antisymmetric  $\varepsilon$  symbol and the Grassmannian nature of the quark fields. Here the  $i$ -th index of  $abc$  and  $j$ -th index of  $def$  are interchanged in  $(abc, def)[i, j]$ . For example,  $(\Gamma_1, \Gamma_2)[1, 1] = \alpha_2\beta_1\gamma_1, \alpha_1\beta_2\gamma_2$  or  $(\Gamma_1, \Gamma_2)[2, 1] = \alpha_1\alpha_2\gamma_1, \beta_1\beta_2\gamma_2$ . Note that the interchange of indices occurs simultaneously for both.

For a given set of Dirac and flavor indices the initial set of operators may be quite large. The determination of an independent basis and the diagonalization of the renormalization constant matrix  $Z$  is then more conveniently done using algebraic computer programs written in Mathematica or Maple.

Although the NBS wave function is always dominated by the operator with the largest value of  $\beta = \beta_C$ , for the potential this is only the case if  $\beta_C \neq 0$ . The potential is repulsive at short distances if  $\beta_C < 0$  and attractive if  $\beta_C > 0$ . However if  $\beta_C = 0$  the leading term in the potential is governed by the next largest non-zero anomalous dimension, and the sign of the potential requires non-perturbative additional information. That there are operators with  $\beta_C = 0$  is clear; e.g. operators of the form  $B_{\alpha[\beta, \alpha]}^{ffg} B_{\hat{\alpha}[\hat{\beta}, \hat{\alpha}]}^{ggf}$  where  $\alpha, \beta$  have the same chirality and  $\hat{\alpha}, \hat{\beta}$  the opposite chirality, since there is no contribution from diagrams where the gluon line joins quarks in the different baryon operators.

We have carried out the program above for the case of 2-baryon wave functions involving 3 different flavors of quarks and also for 3-baryon wave functions. The main results from these analyses are presented in the next subsection.

### 3.2. Results

We have considered the following four problems: short-distance interaction between two nucleons,<sup>18</sup> between two octet baryons,<sup>20</sup> among three nucleons<sup>21</sup> and finally among three octet baryons.<sup>22</sup> In all these cases we mainly concentrated on the question of the existence of a repulsive (or attractive) core of the interaction potential.

#### 3.2.1. 2-body forces

The technical part of the computation<sup>18</sup> for these cases consists of three main steps: the enumeration of independent (taking into account the identities (15)) local gauge invariant 6-quark operators, calculation of the spectrum of 1-loop anomalous dimensions (by diagonalizing the 1-loop mixing matrix) and finally checking whether a given operator appears already at tree level in the OPE. We found that all 1-loop anomalous dimension eigenvalues are, when multiplied by  $48\pi^2$ , even integers. This suggests that there is a rationally related natural basis in which the mixing matrix is automatically diagonal but we were unable to find a simple method to find this basis.

##### *2-nucleon potential (2 flavors)*<sup>18</sup>

The most important property of the spectrum in this case is that for all operators

$$\gamma_A \leq 2\gamma_N \quad (16)$$

hence  $\beta_A$ , the leading power of the running coupling is non-positive. Almost all operators have negative  $\beta_A$  indicating repulsive behavior, but as explained above, there are also operators with the equality sign in (16). In these cases whether the leading behavior corresponds to attraction or repulsion cannot unfortunately be decided using perturbation theory alone. In the short distance limit the potential behaves as

$$V(\mathbf{x}) \sim R \frac{\bar{g}^{2(1-\beta')}(|\mathbf{x}|)}{x^2} \quad (17)$$

in these cases, where  $\beta' < 0$  corresponds to the subleading operator and  $R$  is the ratio of the matrix elements of the leading and subleading operators sandwiched between the vacuum and the given 2-nucleon state. The latter can only be calculated non-perturbatively. Since we are only interested in the *sign* of this quantity, we were able to use a simple effective model to conclude<sup>18</sup> that this sign is always positive leading to repulsion in all cases.

##### *2-baryon potential (3 flavors)*<sup>20</sup>

8 *S. Aoki, J. Balog, T. Doi, T. Inoue, P. Weisz*

Table 1. List of channels with 1-loop anomalous dimensions greater than  $2\gamma_N$ ; others can be obtained by symmetry transforms of the Dirac indices  $1 \leftrightarrow 2, 3 \leftrightarrow 4$  or  $(1, 2) \leftrightarrow (3, 4)$ .

Dirac structure	$48\pi^2\gamma_A$	SU(3) representation
112334	42	1
111222	36	1
112234	36	1
111234	32	$1 \oplus 8$
112234	32	$1 \oplus 8$

The tensor product of two octets can be decomposed under SU(3) as

$$8 \otimes 8 = 1_s \oplus 8_s \oplus 27_s \oplus 8_a \oplus 10_a \oplus \overline{10}_a, \quad (18)$$

where the subscript  $s(a)$  indicates symmetry (antisymmetry) under the interchange of the two octet representations. We considered local 6-quark operators with flavor content  $uuddss$  because such operators represent all multiplets in the above decomposition. Again, most operators have  $\gamma_A \leq 2\gamma_N$  but there are also attractive cases, operators with  $\gamma_A > 2\gamma_N$  (see Table 1). These all belong to the representations  $1_s$ ,  $8_s$  and  $8_a$ , consistent with what we found for the 2-nucleon case, since 2-nucleon states belong to the  $\overline{10}_a$  and  $27_s$  SU(3) representations. Finally we found that all operators with  $\gamma_A > 2\gamma_N$  appear already at tree level in the OPE of two nucleon fields.

### 3.2.2. 3-body forces

As explained in the introduction, collective phenomena in nuclear physics cannot be described using only 2-body potentials. In particular, the existence of massive neutron stars suggests that also the 3-nucleon potential has a repulsive core. To study 3-body forces with our method we introduce the 3-particle generalization of the NBS wave function (1)

$$\varphi_{\alpha\beta\gamma}^E(\mathbf{r}, \boldsymbol{\rho}) = \langle 0 | T \{ B_\alpha(\mathbf{x}_1, 0) B_\beta(\mathbf{x}_2, 0) B_\gamma(\mathbf{x}_3, 0) \} | 3B, E \rangle_{\text{in}}, \quad (19)$$

where for transparency we suppressed momentum and helicity dependence. Here  $B_\alpha$  is the baryon-octet generalization of the nucleon doublet field appearing in (1) and  $3B$  is an appropriate 3-baryon state with energy  $E$ . In the argument of the 3-body NBS wave function we use Jacobi coordinates  $\mathbf{r} = \mathbf{x}_1 - \mathbf{x}_2$  and  $\boldsymbol{\rho} = [\mathbf{x}_3 - (\mathbf{x}_1 + \mathbf{x}_2)/2]/\sqrt{3}$ .

In the local potential approximation we have

$$\left[ -\frac{1}{m_N} \left( \nabla_r^2 + \frac{1}{4} \nabla_\rho^2 \right) + \mathcal{V}_{3B} \right] \varphi_{\alpha\beta\gamma}^E = E \varphi_{\alpha\beta\gamma}^E. \quad (20)$$



This defines the total 3-baryon potential  $\mathcal{V}_{3B}$  and the true 3-baryon potential  $V_{3B}$  is given by the potential excess

$$\mathcal{V}_{3B}(\mathbf{r}, \boldsymbol{\rho}) = \sum_{i < j} V_{2B}(\mathbf{x}_i - \mathbf{x}_j) + V_{3B}(\mathbf{r}, \boldsymbol{\rho}), \quad (21)$$

where  $V_{2B}$  is the 2-baryon potential discussed above.

In the UV limit, i.e. when  $s = \sqrt{\mathbf{r}^2 + \boldsymbol{\rho}^2} \rightarrow 0$  we can use the OPE method to calculate the leading behavior of the wave function (19) analogously to the 2-body case but here we have to consider local gauge invariant 9-quark operators. We have carried out the anomalous dimension analysis both in the 3-nucleon case and the most demanding 3-baryon case.

### *3-nucleon potential (2 flavors)<sup>21</sup>*

The most striking feature of the spectrum in this case is that for *all* operators

$$\gamma_A < 3\gamma_N. \quad (22)$$

Here again operators with the largest anomalous dimension are present in the 3-nucleon OPE at lowest order and we conclude that the total local potential in this case behaves asymptotically as

$$\mathcal{V}_{3N}(\mathbf{r}, \boldsymbol{\rho}) \sim \frac{\bar{g}^2(s)}{s^2} \quad (23)$$

(up to a positive constant). Since at short distances this dominates the 2-nucleon potential which behaves as given in (17) it follows that the genuine 3-body potential  $V_{3B}$  introduced above is responsible for the short-distance repulsion.

We note that showing the presence of a repulsive core in the 3-nucleon case is the most important result of our perturbative considerations. Universal repulsion follows unambiguously from (22) without having to rely on any model-dependent results.

We also note that one can observe from the calculated pattern of the spectrum of 1-loop anomalous dimensions that the Pauli exclusion principle is at work here: increasing the number of quarks while keeping the number of flavors fixed makes repulsion stronger while increasing the number of flavors and fixing the number of quarks brings in some attractive channels.

### *3-baryon potential (3 flavors)<sup>22</sup>*

In this case the SU(3) decomposition is

$$8 \otimes 8 \otimes 8 = 64 \oplus (35 \oplus \overline{35})_2 \oplus 27_6 \oplus (10 \oplus \overline{10})_4 \oplus 8_8 \oplus 1_2 \quad (24)$$

and one can show that it is sufficient to work with the flavor content  $uuudddsss$  since all representations on the right hand side of the above formula occur in this flavor sector.

The 3-baryon case is the most demanding technically. There are many Dirac index configurations to be considered and for some of them the dimension of the problem is quite large: with Dirac index structure 111223344 for example there are

10 *S. Aoki, J. Balog, T. Doi, T. Inoue, P. Weisz*

Table 2. List of 3-baryon channels with anomalous dimensions greater than or equal to  $3\gamma_N$ . Only operators present at tree level are listed.

Dirac structure	$48\pi^2\gamma_A$	SU(3) representation
111223344	48	8
	44	1, 8
	42	1, 8
	36	8, 10, $\overline{10}$
111333224	44	1, 8
111222334	48	8
	44	1
111133442	42	1, 8
111122334	44	1

originally 14130 operators and this number is reduced to 1518 after imposing the 9-quark generalization of the identities (15). After performing the diagonalization in all Dirac sectors we found that in the 3-baryon case, although the vast majority of the eigenvalues are  $< 3\gamma_N$ , there are also some attractive channels. We enumerate these cases in Table 2 (only operators appearing at tree level in the OPE are listed).

Our calculations allow us to determine the leading UV behavior of the total 3-baryon potential  $\mathcal{V}_{3B}$ . However, to draw any conclusion concerning the UV limit of the genuine 3-body potential  $V_{3B}$  is difficult since comparing the results in Tables 1 and 2 we see that in some cases the 2-body forces are dominant, moreover there are also cases where there is cancellation between two different 2-body contributions.

#### 4. Results from lattice QCD and comparisons with OPE predictions

In lattice QCD simulations with the spatial volume  $L^3$ , the NBS wave function can be extracted from the 4-point correlation function,<sup>6,8</sup> which is given, for example, in the case of the  $NN$  system at  $t > t_0$  by

$$\mathcal{G}_{\alpha\beta}(\mathbf{x}, t - t_0) \equiv \langle 0 | T \{ N_\alpha(\mathbf{r}, t) N_\beta(\mathbf{r} + \mathbf{x}, t) \} \overline{\mathcal{J}}_{NN}(t_0) | 0 \rangle \quad (25)$$

$$= \sum_{n, s_1, s_2} A(\mathbf{k}_n, s_1, s_2) \varphi_{\alpha\beta}^{\mathbf{k}_n, s_1, s_2}(\mathbf{x}) e^{-W_{\mathbf{k}_n}(t-t_0)} + \dots \quad (26)$$

$$\longrightarrow A(\mathbf{k}_0, s_1, s_2) \varphi_{\alpha\beta}^{\mathbf{k}_0, s_1, s_2}(\mathbf{x}) e^{-W_{\mathbf{k}_0}(t-t_0)}, \quad t \gg t_0, \quad (27)$$

with the matrix element  $A(\mathbf{k}_n, s_1, s_2) = {}_{\text{in}}\langle NN, \mathbf{k}_n, s_1, s_2 | \overline{\mathcal{J}}_{NN}(0) \rangle$ , where  $\overline{\mathcal{J}}_{NN}(t_0)$  is some source operator which can create states  $|NN, \mathbf{k}_n, s_1, s_2\rangle_{\text{in}}$ , and the ellipses represent inelastic contributions from intermediate states other than  $NN$ . In our numerical simulations, we have mainly used a wall source with the Coulomb gauge fixing only at  $t = t_0$ .<sup>8</sup> The large  $t - t_0$  necessary to achieve ground state saturation

in the last line causes some difficulties in numerical simulations. The signal-to-noise ratio for nucleon 4-pt functions behaves asymptotically for large  $t$  as<sup>25,26</sup>  $\left(\frac{\mathcal{S}}{\mathcal{N}}\right) \sim e^{-2(m_N - 3m_\pi/2)t}$ , where  $m_N$  and  $m_\pi$  are the nucleon and pion masses, respectively. This problem becomes worse as we decrease the pion mass toward its physical value. Furthermore, as we increase the volume, the splitting between the ground state and the 1st excited state for the 2 nucleon system becomes smaller as  $\Delta E \simeq \frac{\mathbf{k}_{\min}^2}{m_N} = \frac{1}{m_N} \left(\frac{2\pi}{L}\right)^2$ . If  $L \simeq 5fm$  and  $m_N \simeq 1$  GeV,  $\Delta E \simeq 62\text{MeV} \simeq 1/(3.2\text{fm})$ , which requires  $t \gg (\Delta E)^{-1} \simeq 3.2$  fm for ground state saturation. The behavior of statistical noise in the above, however, makes the signals very poor at such large  $t$  for the two nucleon system.

Recently, an improved extraction of the NBS wave function has been proposed to overcome the above difficulties.<sup>27</sup> We first define the normalized 4-point correlation function as

$$R(\mathbf{x}, t) \equiv \mathcal{G}(\mathbf{x}, t)/(e^{-m_N t})^2 \simeq \sum_{n, s_1, s_2} A(\mathbf{k}_n, s_1, s_2) \varphi^{\mathbf{k}_n, s_1, s_2}(\mathbf{x}) e^{-\Delta W_{\mathbf{k}_n} t} \quad (28)$$

where  $\Delta W_{\mathbf{k}} = 2\sqrt{m_N^2 + \mathbf{k}^2} - 2m_N$ . Using an identity  $\Delta W_{\mathbf{k}} = \mathbf{k}^2/m_N - (\Delta W_{\mathbf{k}})^2/(4m_N)$  and neglecting inelastic contributions, we arrive at the time-dependent Schrödinger-like equation

$$\left\{ -H_0 - \frac{\partial}{\partial t} + \frac{1}{4m_N} \frac{\partial^2}{\partial t^2} \right\} R(\mathbf{x}, t) = \int d^3y U(\mathbf{x}, \mathbf{y}) R(\mathbf{y}, t) \quad (29)$$

$$\simeq V(\mathbf{x}) R(\mathbf{x}, t) + \dots, \quad (30)$$

which shows that the same  $U(\mathbf{x}, \mathbf{y})$  in eq. (4) can be obtained from  $R(\mathbf{x}, t)$ , where in the last line the derivative expansion is employed. An advantage of this extraction is that ground state saturation is not required for  $R(\mathbf{x}, t)$  to satisfy eq. (29) or eq. (30). For this method to work,  $t$  has to be large enough such that elastic contributions dominate  $R(\mathbf{x}, t)$ .

#### 4.1. Nucleon-Nucleon potentials

We first show the parity-even NN potentials at the leading order in the derivative expansion in Fig. 1, where the central potential for the spin-singlet sector  $V_c^{I=1}(r) \equiv V_0^{I=1}(r) - 3V_\sigma^{I=1}(r)$ , the central potential for the spin-triplet sector  $V_c^{I=0}(r) \equiv V_0^{I=0}(r) + V_\sigma^{I=0}(r)$  and the tensor potential for the spin-triplet sector  $V_T^{I=0}(r)$  are plotted as a function of  $r$  by blue, green and red symbols, respectively.<sup>28</sup> The results in the left figure have been obtained using PACS-CS gauge configurations in the 2+1 flavor QCD at  $m_\pi \simeq 701$  MeV and the lattice spacing  $a \simeq 0.091$  fm on  $32^3 \times 64$  lattice,<sup>29</sup> while those in the right figure have been obtained in quenched QCD at  $m_\pi \simeq 731$  MeV and  $a \simeq 0.137$  fm on a  $32^4$  lattice.

The central potentials for both spin-singlet and spin-triplet sectors have repulsive cores, which confirm eq. (17) with positive  $R$ , while the tensor potential is less

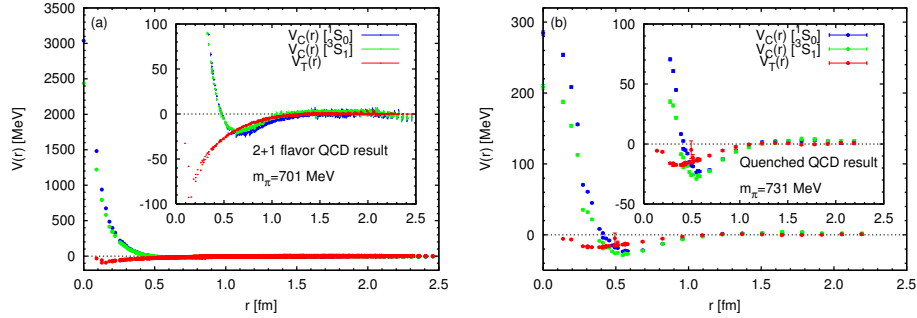
12 *S. Aoki, J. Balog, T. Doi, T. Inoue, P. Weisz*


Fig. 1. Central and tensor potentials in 2+1 flavor QCD at  $m_\pi = 701$  MeV by the improved method (left) and in quenched QCD at  $m_\pi = 731$  MeV by the conventional method(right).

singular at short distance, in accordance with the fact that short distance contributions do not exist at the leading order of PT.<sup>18</sup> Note however that the central potentials are finite at the origin in contrast to the divergent behavior predicted by the OPE analysis, probably due to the artifact of non-zero lattice spacing. It is therefore important to show the appearance of the expected divergent behavior in future numerical simulations, by taking the continuum limit. We also observe that the repulsive cores and the tensor potential become significantly enhanced in the 2+1 flavor QCD.

#### 4.2. Baryon interactions in the flavor $SU(3)$ limit

The figures in Fig. 2 show the leading order BB potential from full QCD simulations in the flavor  $SU(3)$  limit at the pseudo-scalar meson mass  $M_{PS} = 469(1)\text{MeV}$  and  $a = 0.121(2)\text{fm}$ ,<sup>30</sup> where the central potentials (red) in the spin-singlet sector are given for the 27,  $8_s$  and 1 irreducible representations of  $SU(3)$ , from left to right in the 1st row, while the central and tensor potentials in the spin-triplet sector are given for  $\overline{10}$ , 10 and  $8_a$  in the 2nd row.

The OPE analysis in the previous section predicts that, while the central potentials in the 27,  $\overline{10}$  and 10 representations have a repulsive core, attractive interactions dominate at short distances for the central potentials in the 1,  $8_s$  and  $8_a$  representations. Indeed, the central potential in the singlet representation,  $V^{(1)}$ , shows attraction at short distance in Fig. 2, which leads to the bound H-dibaryon in this channel.<sup>16</sup> The OPE analysis correctly predicts the attractive interaction at short distance in the singlet representation. On the other hand, while the repulsion at short distance becomes weaker in the  $8_a$  representation, it becomes strongest among all 6 representations in the  $8_s$  representation. The OPE analysis does not reproduce these repulsions.

This puzzle may be resolved by observing<sup>20</sup> that there is no 6-quark operator in the  $8_s$  channel in the nonrelativistic limit and therefore the corresponding nonperturbative matrix elements must be small. Although the channel remains attractive

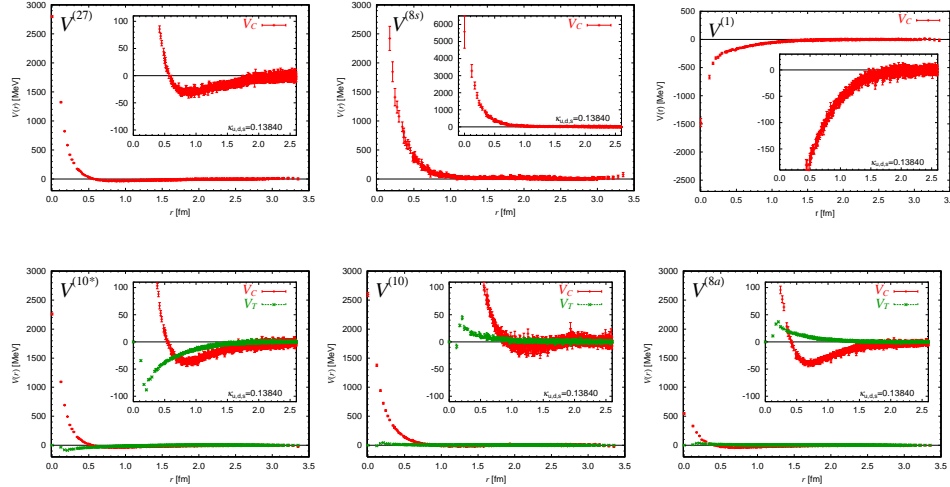


Fig. 2. Potentials of baryon-baryon S-wave interaction in the flavor  $SU(3)$  limit, labeled by the flavor irreducible representation. These are obtained at the pseudo-scalar meson mass of 469 MeV by the improved method.

at extremely short distances, in the range between 0.1 fm and 0.5 fm relevant for lattice simulations subleading operators, which are repulsive, dominate. Note that a valence quark model with gluon exchange<sup>31,32</sup> can reproduce the correct pattern of the short distance behavior of potentials observed in lattice QCD simulations including the attraction in the singlet channel.

### 4.3. Three-nucleon force

The three-nucleon force (3NF) has been calculated in the linear setup with  $\rho = 0$ , where three nucleons are aligned linearly with equal spacing  $r_2 = |\mathbf{r}|/2$ , in 2-flavor QCD at  $a \simeq 0.156$  fm and  $m_\pi \simeq 1.13$  GeV on a  $16^3 \times 32$  lattice.<sup>17</sup> In the left of Fig. 3, we give the 3NF  $V_{3N}(\mathbf{r}, \rho)$  at  $\rho = 0$  as a function of  $r_2$ , which are obtained by the improved method in eqs. (29, 30) for the 3NF<sup>33,34</sup> where  $R(\mathbf{x}, t)$  for two nucleons is replaced with  $R(\mathbf{r}, \rho, t)$  for three nucleons. The results from the different sink times are consistent with each other within statistical errors. We observe an indication of repulsive 3NF at short distance, which is consistent with the prediction by the OPE analysis that 3NF is universally repulsive. As in the case of the 2NF, the potential is finite at the origin due to the non-zero lattice spacing in lattice QCD simulations. It is therefore important to further investigate the short distance behavior as a function of the lattice spacing  $a$ .

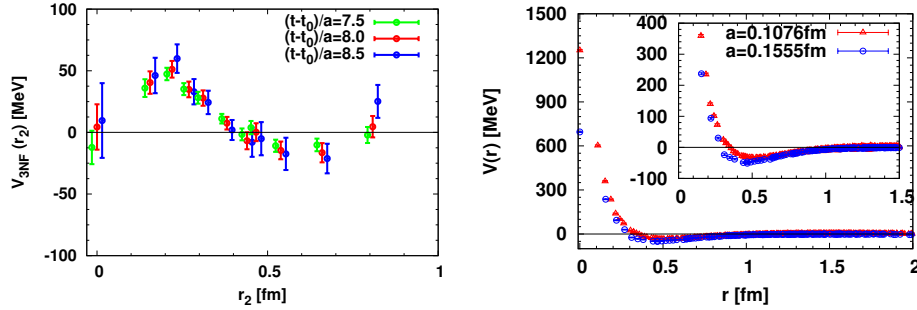
14 *S. Aoki, J. Balog, T. Doi, T. Inoue, P. Weisz*


Fig. 3. (Left) The 3NF  $V_{3N}(\mathbf{r}, \rho)$  at  $\rho = 0$  as a function of  $r_2 = |\mathbf{r}|/2$ , obtained by the improved method at  $(t - t_0)/a = 7.5$  (green), 8 (red) and 8.5 (blue) at  $m_\pi \simeq 1.13$  GeV and  $a \simeq 0.156$  fm. (Right) The spin-singlet central potential in the 2-flavor QCD with  $m_\pi \simeq 1.13$  GeV as a function of  $r$  at  $a \simeq 0.108$  fm (red) and 0.156 fm (blue).

## 5. Conclusions and discussions

In this article, we have reviewed the recent activities to determine the short distance behavior of potentials among baryons, which are defined through the NBS wave function in the HAL QCD method. We can determine the short distance behaviors of the NBS wave functions and thus the corresponding potentials, employing the OPE (operator product expansion) and the RG analysis analytically in perturbation theory of QCD, thanks to its asymptotic freedom.

The most notable predictions from the OPE analysis are (1) an existence of the repulsive cores for the two nucleon potentials with the use of a simple effective model for the ratio of the matrix elements, (2) an appearance of the attractive core, instead of the repulsive one, for the flavor singlet channel in the 3-flavor QCD, and (3) an existence of universal repulsion at short distance for the 3NF without relying on any non-perturbative inputs. These 3 results more or less agree with the behaviors of the corresponding potentials obtained in lattice QCD simulations, except the lattice potentials are always finite at the origin due to the lattice artifacts. There are, however, some disagreements between the OPE analysis and lattice QCD results, which are probably caused by the effects of the neglected subleading terms in the OPE analysis at not asymptotically small distances.

The above success of the OPE analysis suggests that the repulsion among baryons at short distance may be explained by the combination of the Pauli suppression principle among quarks and the one-gluon exchange between quarks<sup>b</sup>. Indeed in the OPE analysis, the tendency of repulsions become stronger for more numbers of quarks, while it becomes weaker for a larger number of valence flavors with the total number of quarks fixed. Since the OPE analysis also predicts forms of the repulsive/attractive cores as a function of distances, it is very important and in-

<sup>b</sup>The valence quark model with gluon exchange mentioned before relies on these properties.<sup>31, 32</sup>

interesting in the future to confirm them in lattice QCD simulations by taking the continuum limit. The right of Fig. 3 shows our very preliminary result for a comparison of the spin-singlet central potential between two lattice spacings,  $a \simeq 0.108$  fm(red) and 0.156 fm(blue). We indeed observe an expected behavior that the repulsive core increases as we decrease the lattice spacing. More data and analysis in this direction will be required to determine the  $r$  dependence of the repulsive cores.

### Acknowledgements

We would like to thank all members of HAL QCD collaboration for researches discussed in this report. S. A. is supported in part by Grant-in-Aid for Scientific Research on Innovative Areas (No. 2004: 20105001,20105003) and by SPIRE (Strategic Program for Innovative Research). T.D. is supported in part by MEXT Grant-in-Aid for Young Scientists (B) (24740146). T.I. is supported in part by Grant-in-Aid for Scientific Research(C) 23540321. This work was also supported in part by the Hungarian National Science Fund OTKA (under K83267). S. A. and J. B. would like to thank the Max-Planck-Institut für Physik for its kind hospitality during their stay for a part of this research.

### References

1. M. Taketani et al., Prog. Theor. Phys. Suppl. **39**, 1-346 (1967), N. Hoshizaki et al., *ibid.* **42**, 1-159 (1968).  
G. E. Brown and A. D. Jackson, *Nucleon-nucleon Interaction*, (North-Holland, Amsterdam, 1976).  
R. Machleidt, Adv. Nucl. Phys. **19**, 189 (1989).  
R. Machleidt and I. Slaus, *J. Phys.* **G27**, R69 (2001).
2. H. Yukawa, Proc. Math. Phys. Soc. Japan, **17**, 48 (1935).
3. R. Jastrow, Phys. Rev. **81**, 165 (1951).
4. S. Nishizaki, T. Takatsuka and Y. Yamamoto, Prog. Theor. Phys. **108**, 703 (2002).  
T. Takatsuka, S. Nishizaki and R. Tamagaki, Prog. Theor. Phys. Suppl. **174**, 80 (2008).
5. P. Demorest, T. Pennucci, S. Ransom, M. Roberts and J. Hessels, Nature **467**, 1081 (2010) [arXiv:1010.5788 [astro-ph.HE]].
6. N. Ishii, S. Aoki and T. Hatsuda, Phys. Rev. Lett. **99**, 022001 (2007) [arXiv:nucl-th/0611096].
7. S. Aoki, T. Hatsuda and N. Ishii, Comput. Sci. Dis. **1**, 015009 (2008) [arXiv:0805.2462 [hep-ph]].
8. S. Aoki, T. Hatsuda and N. Ishii, Prog. Theor. Phys. **123**, 89(2010) [arXiv:0909.5585 [hep-lat]].
9. N. Ishii, S. Aoki and T. Hatsuda, PoS LATTICE2008, 155 ( 2008) [arXiv:0903.5497 [hep-lat]].
10. K. Murano, N. Ishii, S. Aoki and T. Hatsuda, Prog. Theor. Phys. **125**, 1225 (2011) [arXiv:1103.0619 [hep-lat]].
11. H. Nemura, N. Ishii, S. Aoki and T. Hatsuda, Phys. Lett. B **673**, 136 (2009) [arXiv:0806.1094 [nucl-th]].
12. H. Nemura and f. H. Q. Collaboration, arXiv:1203.3320 [hep-lat].
13. K. Sasaki [for HAL QCD Collaboration], PoS LATTICE **2010**, 157 (2010) [arXiv:1012.5685 [hep-lat]].

16. S. Aoki, J. Balog, T. Doi, T. Inoue, P. Weisz
14. Y. Ikeda [for HAL QCD Collaboration], arXiv:1111.2663 [hep-lat].
  15. T. Inoue *et al.* [HAL QCD collaboration], Prog. Theor. Phys. **124**, 591 (2010) [arXiv:1007.3559 [hep-lat]].
  16. T. Inoue *et al.* [HAL QCD Collaboration], Phys. Rev. Lett. **106**, 162002(2011) [arXiv:1012.5928 [hep-lat]].
  17. T. Doi, S. Aoki, T. Hatsuda, Y. Ikeda, T. Inoue, N. Ishii, K. Murano and H. Nemura *et al.*, Prog. Theor. Phys. **127**, 723 (2012) [arXiv:1106.2276 [hep-lat]].
  18. S. Aoki, J. Balog and P. Weisz, JHEP05, 008 (2010) [arXiv:1002.0977 [hep-lat]].
  19. S. Aoki, J. Balog and P. Weisz, PoS LAT2009, 132 (2009) [arXiv:0910.4255 [hep-lat]].
  20. S. Aoki, J. Balog and P. Weisz, JHEP09, 083 (2010) [arXiv:1007.4117 [hep-lat]].
  21. S. Aoki, J. Balog and P. Weisz, New J. Phys. **14** (2012) 043046 [arXiv:1112.2053 [hep-lat]].
  22. S. Aoki, J. Balog and P. Weisz, Prog. Theor. Phys. **128**, 1269 (2012) [arXiv:1208.1530 [hep-lat]].
  23. N. Ishizuka, PoS LAT2009, 119 (2009).
  24. R. Tamagaki and W. Watari, Prog. Theor. Phys. Suppl. **39**, 23 (1967).
  25. G. Parisi, Phys. Rept. **103**, 203 (1984).
  26. G. P. Lepage, in *From Actions to Answers: Proceedings of the TASI 1989*, edited by T. Degrand and D. Toussaint (World Scientific, Singapore, 1990).
  27. N. Ishii *et al.* [HAL QCD Collaboration], Phys. Lett. B **712**, 437 (2012) [arXiv:1203.3642 [hep-lat]].
  28. N. Ishii [PACS-CS and HAL-QCD Collaborations], PoS LAT **2009**, 019 (2009) [arXiv:1004.0405 [hep-lat]].
  29. S. Aoki *et al.* [PACS-CS Collaboration], Phys. Rev. D **79**, 034503 (2009) [arXiv:0807.1661 [hep-lat]].
  30. T. Inoue *et al.* [HAL QCD Collaboration], Nucl. Phys. A **881**, 28 (2012) [arXiv:1112.5926 [hep-lat]].
  31. M. Oka, K. Shimizu and K. Yazaki, Phys. Lett. B **130**, 365 (1983).
  32. M. Oka, K. Shimizu and K. Yazaki, Nucl. Phys. A **464**, 700 (1987).
  33. T. Doi [HAL QCD Collaboration], arXiv:1212.1606 [hep-lat].
  34. T. Doi [HAL QCD Collaboration], PoS LATTICE **2012**, 009 (2012) [arXiv:1212.1572 [hep-lat]].